JACS
JOURNAL OF THE AMERICAN CHEMICAL SOCIETY

Article

Green-Solvent-Processable, Dopant-Free Hole-Transporting Materials for Robust and Efficient Perovskite Solar Cells

Junwoo Lee, Mahdi Malekshahi Byranvand, Gyeongho Kang, Sung Y. Son, Seulki Song, Guan-Woo Kim, and Taiho Park

J. Am. Chem. Soc., **Just Accepted Manuscript** • DOI: 10.1021/jacs.7b04949 • Publication Date (Web): 16 Aug 2017

ACS Publications

Journal of the American Chemical Society is published by the American Chemical Society. 1155 Sixteenth Street N.W., Washington, DC 20036

Green-Solvent-Processable, Dopant-Free Hole-Transporting Materials for Robust and Efficient Perovskite Solar Cells

Junwoo Lee,‡ Mahdi Malekshahi Byranvand,‡ Gyeongho Kang, Sung Y. Son, Seulki Song, Guan-Woo Kim, and Taiho Park*

Department of Chemical Engineering, Pohang University of Science and Technology, San 31, Nam-gu, Pohang, Gyeongbuk 790-780, Korea

ABSTRACT: In addition to having proper energy levels and high hole mobility (μ_h) without the use of dopants, hole-transporting materials (HTMs) used in n-i-p-type perovskite solar cells (PSCs) should be processed using green solvents to enable environmentally friendly device fabrication. Although many HTMs have been assessed, owing to the limited solubility of HTMs in green solvents, no green-solvent-processable HTM has been reported to date. Here we report on a green-solvent-processable HTM, an asymmetric D–A polymer (asy-PBTBDT) that exhibits superior solubility even in the green solvent, 2-methylanisole, which is a known food additive. The new HTM is well matched with perovskites in terms of energy levels and attains a high μ_h (1.13×10^{-3} cm^2/Vs) even without the use of dopants. Using the HTM, we produced robust PSCs with 18.3% efficiency (91% retention after 30 days without encapsulation under 50%–75% relative humidity) without dopants; with dopants (bis(trifluoromethanesulfonyl) imide and *t*-butylpyridine, a 20.0% efficiency was achieved. Therefore, it is a first report for a green-solvent-processable hole-transporting polymer, exhibiting the highest efficiencies reported so far for n-i-p devices with and without the dopants.

INTRODUCTION

Following the first use of perovskites as light absorption materials by Miyasaka et al.,[1] perovskite solar cells (PSCs) have been widely considered for use in next-generation solar cells.[2-11] In general, the n-i-p-type PSCs comprise a layering of fluorine-doped tin oxide (FTO), an electron transporting layer (ETL), perovskites, a hole-transporting layer (HTL), and a counter electrode (thus, the n-i-p typology). Tremendous efforts have been expended in the development of new materials (ETLs, perovskites, and HTLs) to improve power conversion efficiency (PCE). Among the various components, the development of new HTLs has proven attractive not only to materials scientists but also to academic and industrial engineers, as the current HTL fabrication involves complicated fabrication steps and processes that affect the work conditions and production cost. 2,2′,7,7′-Tetrakis(N,N-di-p-methoxyphenylamine)-9,9′-spirobifluorene (**Spiro-OMeTAD**) is a common hole-transporting material (HTM) that has been widely employed in the development of PSCs with PCEs up to 22.1%.[12] However, despite its low molecular weight relative to polymeric HTMs, it can only be processed in chlorinated or harmful solvents such as chlorobenzene (CB), dichlorobenzene (DCB), or toluene. To enable environmentally friendly fabrication of PSCs, it will therefore be necessary to find a green-solvent-processable HTM. Numerous other HTMs have been developed,[13-21] including those developed by our group,[22-24] that exhibit high PCE values. For instance, Jen et al., Nazeeruddin et al., Sun et al., and Soek et al. independently reported a crosslinked vinylbenzyl ether-functionalized small molecular HTM (TCTA-BVP) (PCE = 18.3%),[25] dissymmetric fluorene-dithiophene (PCE = 20.2%),[26] and several small molecular and polymeric triarylamine-based HTMs (PCEs = 16.7%–20.8%).[27,28,29] However, these high PCE values were achieved only through processing with halogenated or harmful solvents with severe acute toxicity in human body (see Figure S1 for the respective MSDS hazard symbols: GHS06, GHS07, GHS08, and GHS09). In addition, it was necessary to use polar additives (dopants), such as lithium bis(trifl uoromethanesulfonyl) imide (Li-TFSI), and *t*-butylpyridine (*t*-BP), primarily to control hole mobility (μ_h). However, it is well known (and we have demonstrated) that these dopants exhibit deliquescence, leading to the destruction of device functions.[24] Given this background, the key specifications of an ideal HTM would include (1) a proper energy level, (2) a high μ_h value, (3) no use of dopants, and (4) high solubility in non-harmful solvents in order to produce a green-solvent-processable PSC with a high PCE and long-term stability. As mentioned earlier, many studies have reported high PCEs using various HTMs, including **Spiro-OMeTAD**, with sophisticatedly designed energy levels (criterion 1), high μ_h values (criterion 2), and dopant-free HTMs (criterion 3);[30-38] however, only few of these attained reasonable PCEs (with efficiencies of 16.2%,[39] 16.3%,[40] 16.9%,[41] and 14.5%[42] attained by Yang et al., Grätzel et al., Jen et al., and Marks et al., respectively). It is noticed that, in a p-i-n inverted PSC, Chen et al. reported a truxene-based HTM (Trux-OMeTAD), annealed at 150°C (PCE = 18.6%).[43]

Our group also reported a dopant-free, polymeric HTM (random copolymer (RCP)), achieving a high PCE of 17.3% and long-term stability under a 75% relative humidity (RH) condition.[24] However, all of these HTMs were processed with chlorinated or harmful solvents (and therefore did not meet criterion (4)). The need for green HTMs for PSCs with high efficiency and long-term stability that meet all four of the above mentioned criteria is clear.

Here we report a green-solvent-processable, polymeric HTM comprising benzothiadiazole (BT) and benzo[1,2-b:4,5:b′]dithiophene (BDT) (**asy-PBTBDT** in Figure 1). We design a novel *D* (e-donor)–*A* (e-acceptor)-type conducting polymer to easily obtain appropriate highest occupied molecular orbital (HOMO) and achieve high μ_h,[22] allowing effective hole extraction from perovskites to the HTM and hole transportation through the HTM without the use of Li-TFSI and *t*-BP, respectively.[24] To improve solubility, the length or number of alkyl substituents can, in theory, be increased generally, although as we have demonstrated,[44,45] this can sometimes

result in decreased μ_h. Instead, we adopt asymmetric alkyl substituents on BT units in place of the conventional symmetric alkyl substituent (**PBTBDT**) to produce irregularity within a repeating unit of the polymeric (**asy-PBTBDT**) HTM.[23] The resulting novel polymeric HTM is not only soluble in the various halogenated or harmful solvents mentioned above but also highly soluble in 2-MA (ca. 20 mg/ml), which is used as a food additive (Figure 1 and see Figure S2 for that 2-MA did not destroy a perovskite layer).[46] Based on this, we firstly report a green-solvent-processable HTM, **asy-PBTBDT**. Therefore, it is a first step of replacing harmful solvents in fabrication of perovskites solar cells. This makes it possible to produce highly stable devices with 18.3% and 20.0% without and with the dopants, which are the highest efficiencies reported so far for the n-i-p PSCs using polymer HTMs, employing green solvent.

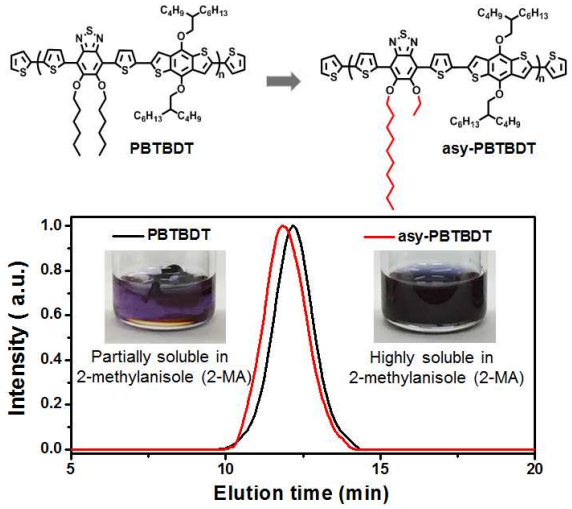

Figure 1. Chemical structures obtained by gel permeation chromatography (GPC) showing their solubilities in 2-methylanisole (2-MA).

RESULTS AND DISCUSSION

Synthesis and characteristics. Detailed synthesis and characterization of **PBTBDT** and **asy-PBTBDT** are described in Figure S3–5 and Note S1 in the Supporting Information. Number-average molecular weights (M_n) and molecular weight distributions (polydispersity indices (PDI)) were determined by GPC using CB as the eluent and a calibration curve of polystyrene standards (Figure 1; also see Table S1). **PBTBDT** is highly soluble in CB, DCB, chloroform, toluene, *o*-xylene, and mesitylene (see Figure S6-7 for the Hansen solubility diagram). Similarly, **asy-PBTBDT** is highly soluble even in 2-MA, although the M_n (ca. 188 *k*Da and 1.55 PDI) of **asy-PBTBDT** is slightly higher than that of **PBTBDT** (180 *k*Da, 1.66 PDI). The solubility of **asy-PBTBDT** measured in this study was ca. 20 mg/mL, which was sufficient to prepare a thick polymer layer on perovskites. The high solubility of **asy-PBTBDT** can be accounted for by the asymmetric alkyl substituents on BT units, which lead to irregularities in the repeating unit of the polymer.

The two polymers exhibited nearly identical intrinsic properties in terms of absorption, oxidation, and thermal degradation as measured using UV–Vis absorption spectroscopy (Figure S8), cyclic voltammetry (Figure S9), thermal gravimetric analysis (Figure S10), and differential scanning calorimetry (DSC) (see insert in Figure S10).

Although the DSC experiments produced no distinctive thermal transitions such as glass transition or heat of melting, the GIWAXS measurements on the polymer films produced weak crystal peaks, as shown in Figure 2a (see also insets in the GIWAXS images). Judging from a comparison of the respective in-plane (100) and out-of-plane (010) scattering peak intensities, the crystallinity of **asy-PBTBDT** film processed with CB (denoted by **asy-PBTBDT$_{CB}$**) was lower than that of **PBTBDT$_{CB}$**. The lower crystallinity in **asy-PBTBDT$_{CB}$** can be attributed to the irregularity of its alkyl chains, enabling superior solubility even in 2-MA. The GIWAXS images of the **asy-PBTBDT** film processed with 2-MA (denoted by **asy-PBTBDT$_{2\text{-}MA}$**) are similar to those of the **asy-PBTBDT$_{CB}$** film (Figure S11). The crystallinity of the **asy-PBTBDT** film was not significantly influenced by the processed solvents.

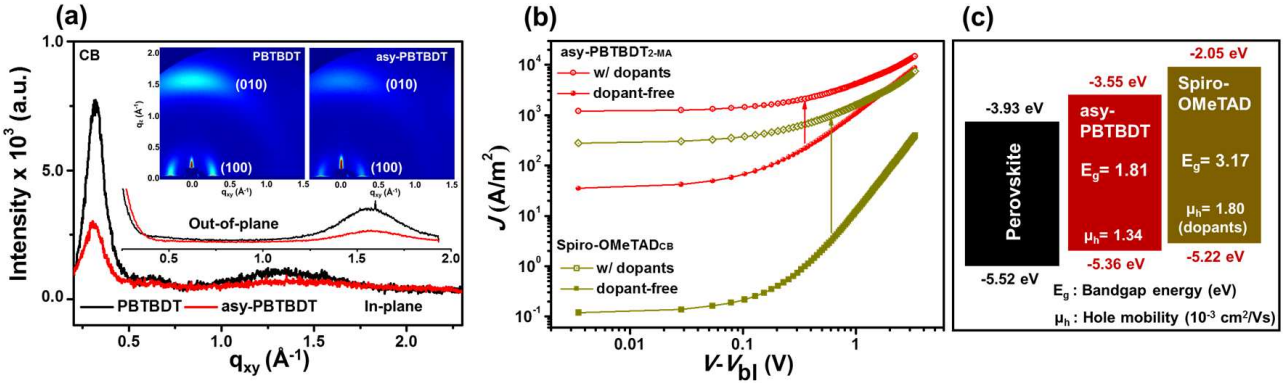

Figure 2. Crystallinity characterization, electronic properties, and energy diagrams. (a) Grazing-incidence wide-angle X-ray scattering (GIWAXS) of **PBTBDT** and **asy-PBTBDT**. **asy-PBTBDT** shows lower crystallinity than that of the control. (b) Dopant-free **asy-PBTBDT$_{2\text{-}MA}$** exhibited hole mobility compatible to doped common **Spiro-OMeTAD$_{CB}$**. (c) Energy diagram obtained using UV–Vis spectrometry and cyclic voltammetry. The energy level of **asy-PBTBDT** is matched to the use of HTMs in PSCs.

Table 1 Summary of the photovoltaic parameters obtained from the best devices. The table lists the average PCE (PCE_{avg}), MPP efficiency (PCE_{MPP}), and current density (J_{MPP}) results for two HTMs prepared using **Spiro-OMeTAD$_{CB}$** with different dopants and for an HTM prepared using **asy-PBTBDT$_{2\text{-}MA}$**. Measurements were performed under AM 1.5 solar illumination. The cell size is 0.09 cm^2.

Device conditions			*J-V curves*					MPP efficiency	
HTM	solvent	dopant	J_{SC} (mA/cm^2)	V_{OC} (V)	*FF* (%)	PCE (PCE$_{avg}$) (%)	PCE$_{avg.hys}$ (%)	J_{MPP} (mA/cm^2)	PCE$_{MPP}$ (%)
asy-PBTBDT$_{2\text{-}MA}$ (R)	2-MA	X	22.4	1.11	73.2	18.3 (17.4)	17.9	20.5	17.4
(F)			21.8	1.10	72.5	17.5			
Spiro-OMeTAD$_{CB}$ (R)	CB	O	22.1	1.11	74.9	18.5 (17.4)	18.1	20.6	17.5
(F)			22.0	1.09	73.5	17.7			
Spiro-OMeTAD$_{CB}$ (R)	CB	X	19.8	0.99	50.4	9.9 (7.7)	9.1	13.4	9.1
(F)			20.1	0.98	42.0	8.2			

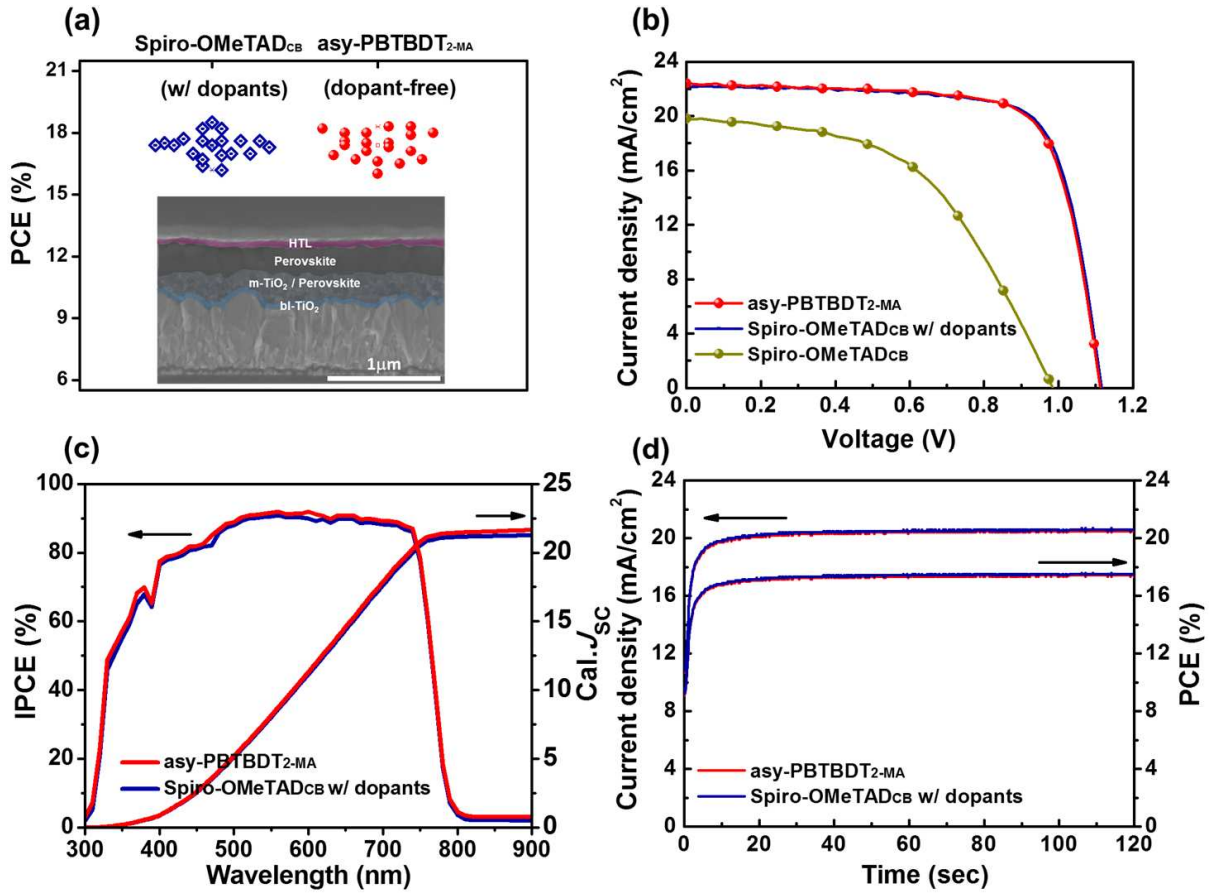

Figure 3. PSC characterization. (a) Dopant-free **asy-PBTBDT$_{2\text{-}MA}$** (red solid points) and doped **Spiro-OMeTAD$_{CB}$** (blue solid points) device statistics taken from measurements of 20 devices with an average PCE of 17.4%. (b) *J–V* curves of the respective PSCs. The dopant-free **asy-PBTBDT$_{2\text{-}MA}$** exhibited performance compatible to that of doped **Spiro-OMeTAD$_{CB}$**. (c) IPCE of devices using dopant-free **asy-PBTBDT$_{2\text{-}MA}$** and doped **Spiro-OMeTAD$_{CB}$**. (d) MPP curves of the champion cells. These values are compatible to the corresponding *J–V* curve results.

Note that in our results, we denote "a polymer film processed with a solvent" as **Polymer$_{solvent}$**, as a processing solvent might influence the properties of the polymer film.

Hole mobility and energy levels. The hole mobility (μ_h) of **asy-PBTBDT** was measured using the space charge limited current method. The μ_h value of the dopant-free **asy-PBTBDT$_{2\text{-}MA\ or\ CB}$** was in the range of 1.13–1.34 × 10^{-3} cm^2/Vs (Figure 2b and Figure S12), which is similar to that of the doped **Spiro-OMeTAD$_{CB}$** containing 2 mM Li-TFSI and 0.07 mM *t*-BP (1.80 × 10^{-3} cm^2/Vs). Note that the μ_h value (ca. 1.40 × 10^{-4} cm^2/Vs) of the dopant-free **Spiro-OMeTAD$_{CB}$** was one order of magnitude lower than that of the doped HTM. Addition of two types of dopants to **asy-PBTBDT$_{2\text{-}MA}$**

$_{or\ CB}$ resulted in significant increases in its μ_h values to 4.71 × 10^{-3} and 4.82 × 10^{-3} cm^2/Vs, respectively, along with effective charge carrier density (Figure S13 and Table S2).

The HOMO and lowest unoccupied molecular orbital of **asy-PBTBDT** were placed at ca. −5.36 and −3.55 eV, respectively (Table S1), based on estimates of the oxidation potential in cyclic voltammograms and the bandgap value (1.81 eV) in the UV–Vis absorption spectra. This energy value was in good agreement with a value (-5.3 eV) obtained from UPS measurement (Figure S14). Based on this range, it would be expected that only perovskite-generated holes could be easily transferred to **asy-PBTBDT** HTL showing higher HOMO level than that of the perovskite (ca. –5.52 eV) (Figure 2c and Figure S15).

Photovoltaic performance. Twenty devices were fabricated using dopant-free **asy-PBTBDT$_{2\text{-}MA}$** (Table 1). The overall PCE values ranged from 16.0% to 18.3% (Figure S16-17), which is comparable to that of conventional control devices employing doped **Spiro-OMeTAD$_{CB}$** (Figure 3a and Figure S18-19). In reverse scanning (scan rate = 0.05 V/s), the best device employing dopant-free **asy-PBTBDT$_{2\text{-}MA}$** reached a PCE of 18.3%, which is equivalent to the results obtained by the best control device employing doped **Spiro-OMeTAD$_{CB}$** (PCE of 18.5%) (Figure 3b). Furthermore, The PCE of 18.3% is the highest value among the n-i-p PSC devices employing dopant-free polymeric HTMs up to date. To confirm the J_{SC} values from the *J–V* curves, the incident photon-to-current efficiencies (IPCE) were measured and then used to calculate the $J_{SC.cal}$ values of 21.6 and 21.3 mA/cm^2 for the dopant-free **asy-PBTBDT$_{2\text{-}MA}$** and the doped **Spiro-OMeTAD$_{CB}$**, respectively, which were both in close agreement with the J_{SC} values from the *J–V* curves (Figure 3c).

The maximum power point (MPP) efficiency (PCE_{MPP}) at each MPP was measured to estimate the device performance under real operational conditions (Figure 3d).[47] The stabilized PCE_{MPP} and photocurrent density (J_{MPP}) of the dopant-free **asy-PBTBDT$_{2\text{-}MA}$** devices were found to be 17.4% and 20.5 mA/cm^2, respectively, which is equivalent to the corresponding values in the doped **Spiro-OMeTAD$_{CB}$** device (Table 1). It was noted that owing to the high *FF* value in the dopant-free **asy-PBTBDT$_{2\text{-}MA}$** device, its stabilized J_{MPP} (20.5 mA/cm^2) approached the J_{SC} value (22.4 mA/cm^2) in its *J–V* curve.

The average efficiency ($PCE_{avg\text{-}hys}$) of the reverse and forward scans for the dopant-free asy-$PBTBDT_{2\text{-}MA}$ was 17.9%, which was similar to that for the doped **Spiro-OMeTAD$_{CB}$** (Figure S20-21). This value was comparable to the corresponding stabilized PCE_{MPP} value (17.4%). The result shows that measurement of the stabilized PCE_{MPP} at an MPP is a potentially highly reliable method to estimate device performance under real operational conditions. Similarly, the PCE for the dopant-free **Spiro-OMeTAD$_{CB}$** was ca. 9.9% (Figure. 3b), which is close to its stabilized PCE_{MPP} value (Figure S22) but much lower than that for the doped **Spiro-OMeTAD$_{CB}$**, primarily owing to the decreased *FF* value in both the scan directions. This result indicates the importance of a high HTL μ_h value to achieve robust photovoltaic performance in this type of solar cell.[24]

The high performance of **asy-PBTBDT$_{2\text{-}MA}$** can be primarily ascribed to its favorable film formability as a result of its high solubility in 2-MA and secondarily to its high μ_h value, which is attained using a green solvent without dopants. It was noted that the solubility of **Spiro-OMeTAD** in 2-MA was not as high as that in CB and that the photovoltaic performances of the dopant-free and doped **Spiro-OMeTAD$_{2\text{-}MA}$** (which met criteria (1, 3, and 4) and (1, 2, and 4), respectively) were slightly poorer than those of the corresponding **Spiro-OMeTAD$_{CB}$** (Figure S23). A ca. 0.14 V_{OC} value difference would be expected between two devices using doped **Spiro-OMeTAD$_{CB}$** and dopant-free **asy-PBTBDT$_{CB}$** based on the energy levels shown in Figure 2c, as the HOMO level of **asy-PBTBDT** (−5.36 eV) is deeper than that of **Spiro-OMeTAD** (−5.22 eV).[27] However, the HOMO energy level, which can only be measured by cyclic voltammetry without dopants, represents the neutral state of **Spiro-OMeTAD** in this study. Indeed, the V_{OC} value for the dopant-free **Spiro-OMeTAD$_{CB}$** was 0.99 V, which was ca. 0.12 V smaller than that for the doped **Spiro-OMeTAD$_{CB}$**. It is possible that the increased V_{OC} value for doped **Spiro-OMeTAD$_{CB}$** is caused by the so-called p-doping (direct partial oxidization of the central amine in **Spiro-OMeTAD** with Li-TFSI, see Figure S24a),[48] which might lower the HOMO energy level in an actual doped system.

We further investigated the photovoltaic performance of **asy-PBTBDT$_{CB}$** prepared with a conventional processing solvent (CB) in the absence of any dopants (Table 2, Figure S25-26). This type of dopant-free **asy-PBTBDT$_{CB}$** would possess criteria 1, 2, and 3. The PCE, $PCE_{avg.hys}$, and PCE_{MPP} of the device were 17.1%, 16.7%, and 16.6%, respectively (Figure S27).

We noted that the PCE was similar to the value (PCE = 17.3%) obtained from the D–A type of an RCP possessing criteria 1, 2, and 3, as previously reported by our group.[24] However, the PCE from the dopant-free **asy-PBTBDT$_{CB}$** was slightly lower than that of the dopant-free **asy-PBTBDT$_{2\text{-}MA}$** produced in an identical manner (PCE = 18.3%).

Table 2 Summary of the photovoltaic parameters obtained from best devices, showing average PCE (PCE_{avg}), MPP efficiency (PCE_{MPP}), and current density (J_{MPP}). The devices were fabricated using different types of **asy-PBTBDT** using different solvents and dopants. Measurements were performed under AM 1.5 solar illumination. The cell size is 0.09 cm^2.

Device conditions			***J-V curves***					**MPP efficiency**	
HTM	solvent	dopant	J_{SC} (mA/cm^2)	V_{OC} (V)	*FF* (%)	PCE (PCE_{avg}) (%)	$PCE_{avg.hys}$ (%)	J_{MPP} (mA/cm^2)	PCE_{MPP} (%)
asy-PBTBDT$_{CB}$ (R)	CB	X	21.2	1.12	72.3	17.1 (15.9)	16.7	19.5	16.6
(F)			21.1	1.10	70.0	16.2			
asy-PBTBDT$_{2\text{-}MA}$ (R)	2-MA	O	22.8	1.12	79.4	20.0 (19.2)	19.4	21.1	19.0
(F)			22.7	1.06	78.6	18.8			
asy-PBTBDT$_{CB}$ (R)	CB	O	22.2	1.14	79.6	20.0 (19.5)	19.6	21.1	18.9
(F)			22.0	1.12	77.0	19.1			

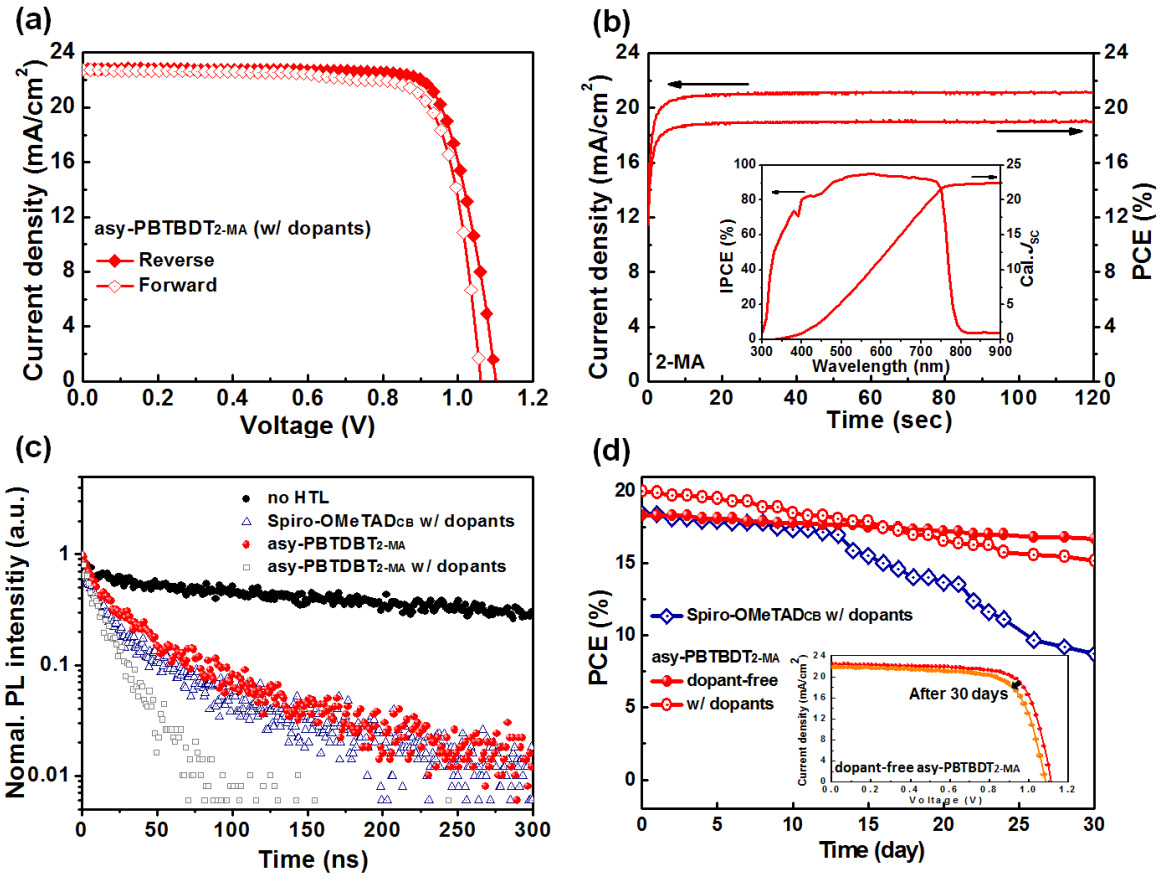

Figure 4. Doped device testing of asy-PBTBDT, hole extraction ability, and long-term stability. (a) Device with doped **asy-PBTBDT$_{2\text{-MA}}$** (red line) shows enhanced PCE owing to increasing μ_h with a low hysteresis phenomenon. (b) The IPCE of doped **asy-PBTBDT$_{2\text{-MA}}$** (red line) confirms the current density predicted by the *J–V* and MPP curves. (c) Pulse width of the excitation source (=70 ps) obtained from the time-resolved photoluminescence measurement of glass/perovskite/HTMs samples. (d) Long-term stability test: devices with dopant-free **asy-PBTBDT$_{2\text{-MA}}$** (red filled circle line) cells, with doped cells (open red circle line), and the device with doped **Spiro-OMeTAD$_{CB}$** (open blue diamond line) were stored at 50%–75% RH and room temperature. Comparison of *J–V* curves between new devices and devices aged 30 days revealed high stability in the dopant-free **asy-PBTBDT$_{2\text{-MA}}$** cell. 2 mM Li-TFSI + 0.07 mM *t*-BP were used as dopants. Noticed that the best efficiency at the first day is obtained with doped asy-PBTBDT, whereas the best stability is obtained with un-doped polymer.

The reason for this discrepancy is not clear, but is likely ascribable to the polarity (δ_p) and boiling temperature (BP) differences between 2-MA (δ_p = 4.7 MPa$^{1/2}$, and BP = 182°C) and CB (δ_p = 3.6 MPa$^{1/2}$, and BP = 131°C) (the cohesive energy density of polarity and boiling temperature were calculated using the Yamamoto-Molecular Break (Y-MB) method in HSPiP).[49] These results suggest that 2-MA can enable better contact between a relatively hydrophobic polymer and a hydrophilic rough perovskite surface.[50,51] As mentioned earlier, the addition of the dopants Li-TFSI and *t*-BP to **asy-PBTBDT$_{2\text{-MA}}$** resulted in a significant increase in its μ_h values to 4.71 × 10^{-3} cm^2/Vs. The effects of these dopants on photovoltaic performance were therefore further studied. Earlier in this study, we reported HTM satisfying criteria 1, 2, and 4 (Table 2). Using 2-MA solvent, The PCE values were of this HTM were enhanced from 18.3% to ca. 20.0%, primarily owing to the resulting increase in the *FF* value (73.2% → 79.4%) (Figure 4a). The efficiency is the highest value among all of the reported polymeric HTMs with dopants. Using the IPCE spectrum, the J_{SC} values were also confirmed (see inset in Figure 4b); given the high PCE$_{avg.hys}$ (19.4%) and *FF* values (Figure 4b), the measured high stabilized PCE$_{MPP}$ (19.0%) and J_{MPP} (21.1 mA/cm^2) were not surprising. Using CB as a processing solvent in the presence of the dopants (thus meeting criteria 1 and 2) (Figure S28), nearly identical efficiencies (PCE = 20.0%, PCE$_{avg.hys}$ = 19.6%, and PCE$_{MPP}$ = 18.9%) and current densities (J_{SC} = 22.2 mA/cm^2, $J_{SC.cal}$ = 22.4 mA/cm^2, J_{MPP} = 21.1 mA/cm^2) were achieved (Table 2); this was also the result of a high μ_h value (4.82 × 10^{-3} cm^2/Vs) achieved without p-doping (Figure S24b).

The excellent photovoltaic performances of the devices employing **asy-PBTBDT$_{2\text{-MA}}$** with and without additives were further investigated using steady-state photoluminescence (SSPL) (see Experimental section and Figure S29 for details). The photoluminescence peak at 760 nm, which originates from excitation of perovskite at 464 nm,

was significantly quenched in perovskite layers covered with doped **Spiro-OMeTAD$_{CB}$**, doped **asy-PBTBDT$_{2\text{-}MA}$**, or dopant-free **asy-PBTBDT$_{2\text{-}MA}$** HTLs, indicating effective hole extraction from the perovskites to the HTLs in all three cases. The HTL quenching rates were measured using time-resolved photoluminescence, producing similar results for the dopant-free **asy-PBTBDT$_{2\text{-}MA}$** and doped **Spiro-OMeTAD$_{CB}$** but a faster quenching rate in the doped **asy-PBTBDT$_{2\text{-}MA}$** (Figure 4c). Identical trends were observed in HTLs processed with CB (See Figure S30-31 for a comparison of the dopant effects on the respective quenching rates).

Finally, non-encapsulated devices were stored under 50%–75% RH conditions to measure long-term stability. The 30-day efficiency of a device processed with green solvent (2-MA) without dopants retained ca. 91% of its initial PCE (Figure 4d) owing to the intrinsic hydrophobicity of the dopant-free **asy-PBTBDT$_{2\text{-}MA}$** (Figure S32). This value was much higher than that for the doped **asy-PBTPBDT$_{2\text{-}MA}$,** which lost approximately 25% of its efficiency over the test period. Furthermore, the doped **Spiro-OMeTAD$_{CB}$** showed that the efficiency remarkably decreases by around 60%. The result is consistent with the results previously reported by our group.[24] Overall, the tests described above confirm that **asy-PBTBDT** is the first reported HTM to possess all four of the following criteria: (1) a proper energy level, (2) a high μ_h value, (3) no use of dopants, and (4) high solubility in non-harmful solvents.

CONCLUSION

In this study, we demonstrated that the asymmetric substituted polymer **asy-PBTBDT** has superior solubility in the edible food additive 2-MA relative to the symmetric polymer (**PBTBDT**) despite the identical carbon numbers in their respective alkyl groups. The μ_h value of dopant-free **asy-PBTBDT$_{2\text{-}MA}$** was found to be ca. 1.13×10^{-3} cm^2/Vs, which is nearly identical to that of doped **Spiro-OMeTAD$_{CB}$** (1.80×10^{-3} cm^2/Vs). Dopant-free **asy-PBTBDT$_{2\text{-}MA}$** processed using a green solvent can be used to fabricate PSCs with high long-term stability and photovoltaic performance (i.e., a PCE of 18.3%). Addition of dopants to **asy-PBTBDT$_{2\text{-}MA}$** significantly improves photovoltaic performance to up to PCE = 20% owing to dopant-induced enhancement of the μ_h. These efficiencies represent the highest values in n-i-p PSCs using robust polymeric HTMs in case of dopant-free and use of dopant, respectively. The approach described in this paper has the potential to commercialize the PSCs by enhancing solubility in green solvent and to further improve photovoltaic performance by increasing HTL μ_h values, which in turn could significantly step up the commercialization pathway of PSCs. This development strategy could also be applied to a variety of polymer-based optoelectronics, including bulk heterojunction solar cells and organic light-emitting or organic field-effect transistors.

ASSOCIATED CONTENT

Supporting Information

The Supporting Information is available free of charge on the ACS Publications website at DOI: xx.xxxx/jacs.xxxxxxx.

Experimental details, synthesis of polymers, device fabrication, and detailed experimental procedures

AUTHOR INFORMATION

Corresponding Author

* taihopark@postech.ac.kr

Author Contributions

‡These authors contributed equally.

Notes

The authors declare no competing financial interest.

ACKNOWLEDGMENT

This work was supported by grants from the Center for Advanced Soft Electronics under the Global Frontier Research Program (Code No. NRF-2012M3A6A5055225) and the National Research Foundation of Korea (NRF) grant (Code No. 2015R1A2A1A10054230) funded by the Korea government (MSIP).

REFERENCES

(1) Kojima, A.; Teshima, K.; Shirai, Y.; Miyasaka, T. *J. Am. Chem. Soc.* **2009**, *131*, 6050-6051.
(2) Park, N.-G. *Mater. Today* **2015**, *18*, 65-72.
(3) Correa-Baena, J.-P.; Abate, A.; Saliba, M.; Tress, W.; Jacobsson, T. J.; Grätzel, M.; Hagfeldt, A. *Energy. Environ. Sci.* **2017**, *10*, 710-727.
(4) Byranvand, M. M.; Song, S.; Pyeon, L.; Kang, G.; Lee, G.-Y.; Park, T. *Nano Energy* **2017**, *10*, 181-187.
(5) Choi, J.; Song, S.; Hörantner, M. T.; Snaith, H. J.; Park, T. *ACS Nano* **2016**, *10*, 6029-6036.
(6) Song, S.; Hörantner, M. T.; Choi, K.; Snaith, H. J.; Park, T. *J. Mater. Chem. A* **2017**, *5*, 3812-3818.
(7) Song, S.; Moon, B. J.; Hörantner, M. T.; Lim, J.; Kang, G.; Park, M.; Kim, J. Y.; Snaith, H. J.; Park, T. *Nano Energy* **2016**, *28*, 269-276.
(8) Manser, J. S.; Christians, J. A.; Kamat, P. V. *Chem. Rev.* **2016**, *116*, 12956-13008.
(9) Ito, S.; Mizuta, G.; Kanaya, S.; Kanda, H.; Nishina, T.; Nakashima, S.; Fujisawa, H.; Shimizu, M.; Haruyama, Y.; Nishino, H. *Phys. Chem. Chem. Phys.* **2016**, *18*, 27102-27108.
(10) Niemann, R. G.; Gouda, L.; Hu, J.; Tirosh, S.; Gottesman, R.; Cameron, P. J.; Zaban, A. *J. Mater. Chem. A* **2016**, *4*, 17819-17827.
(11) Guerrero, A.; You, J.; Aranda, C.; Kang, Y. S.; Garcia-Belmonte, G.; Zhou, H.; Bisquert, J.; Yang, Y. *ACS Nano* **2015**, *10*, 218-224.
(12) Yang, W. S.; Park, B. –W.; Jung, E. H.; Jeon, N. J.; Kim, Y. C.; Lee, D. U.; Shin, S. S.; Seo, J.; Kim, E. K.; Noh, J. H.; Seok, S. I. *Science* **2017**, *356*, 1376-1379.
(13) Reddy, S. S.; Gunasekar, K.; Heo, J. H.; Im, S. H.; Kim, C. S.; Kim, D. H.; Moon, J. H.; Lee, J. Y.; Song, M.; Jin, S. H. *Adv. Mater.* **2015**, *28*, 686-693.
(14) Zhang, J.; Xu, B.; Johansson, M. B.; Hadadian, M.; Correa Baena, J. P.; Liu, P.; Hua, Y.; Vlachopoulos, N.; Johansson, E. M.; Boschloo, G. *Adv. Energy Mater.* **2016**, *6*, 1502536.
(15) Rakstys, K.; Abate, A.; Dar, M. I.; Gao, P.; Jankauskas, V.; Jacopin, G. n.; Kamarauskas, E.; Kazim, S.; Ahmad, S.; Grätzel, M. *J. Am. Chem. Soc.* **2015**, *137*, 16172-16178.
(16) Malinauskas, T.; Saliba, M.; Matsui, T.; Daskeviciene, M.; Urnikaite, S.; Gratia, P.; Send, R.; Wonneberger, H.; Bruder, I.; Graetzel, M. *Energy. Environ. Sci.* **2016**, *9*, 1681-1686.
(17) Xu, B.; Bi, D.; Hua, Y.; Liu, P.; Cheng, M.; Grätzel, M.; Kloo, L.; Hagfeldt, A.; Sun, L. *Energy. Environ. Sci.* **2016**, *9*, 873-877.
(18) Li, M.-H.; Hsu, C.-W.; Shen, P.-S.; Cheng, H.-M.; Chi, Y.; Chen, P.; Guo, T.-F. *Chem. Commun.* **2015**, *51*, 15518-15521.
(19) Cheng, M.; Aitola, K.; Chen, C.; Zhang, F.; Liu, P.; Sveinbjörnsson, K.; Hua, Y.; Kloo, L.; Boschloo, G.; Sun, L. *Nano Energy* **2016**, *30*, 387-397.
(20) Cho, I.; Jeon, N. J.; Kwon, O. K.; Kim, D. W.; Jung, E. H.; Noh, J. H.; Seo, J.; Seok, S. I.; Park, S. Y. *Chem. Sci.* **2017**, *8*, 734-741.
(21) Park, S.; Heo, J. H.; Cheon, C. H.; Kim, H.; Im, S. H.; Son, H. J. *J. Mater. Chem. A* **2015**, *3*, 24215-24220.

(22) Kwon, Y. S.; Lim, J.; Yun, H.-J.; Kim, Y.-H.; Park, T. *Energy. Environ. Sci.* **2014**, *7*, 1454-1460.
(23) Kim, G. W.; Kim, J.; Lee, G. Y.; Kang, G.; Lee, J.; Park, T. *Adv. Energy Mater.* **2015**, *5*, 1500471.
(24) Kim, G.-W.; Kang, G.; Kim, J.; Lee, G.-Y.; Kim, H. I.; Pyeon, L.; Lee, J.; Park, T. *Energy. Environ. Sci.* **2016**, *9*, 2326-2333.
(25) Li, Z.; Zhu, Z.; Chueh, C. C.; Luo, J.; Jen, A. K. Y. *Adv. Energy Mater.* **2016**, *6*, 1601165.
(26) Saliba, M.; Orlandi, S.; Matsui, T.; Aghazada, S.; Cavazzini, M.; Correa-Baena, J.-P.; Gao, P.; Scopelliti, R.; Mosconi, E.; Dahmen, K.-H. *Nat. Energy* **2016**, *1*, 15017.
(27) Jeon, N. J.; Lee, H. G.; Kim, Y. C.; Seo, J.; Noh, J. H.; Lee, J.; Seok, S. I. *J. Am. Chem. Soc.* **2014**, *136*, 7837-7840.
(28) Yang, W. S.; Noh, J. H.; Jeon, N. J.; Kim, Y. C.; Ryu, S.; Seo, J.; Seok, S. I. *Science* **2015**, *348*, 1234-1237.
(29) Xu, B.; Zhang, J.; Hua, Y.; Liu, P.; Wang, L.; Ruan, C.; Li, Y.; Boschloo, G.; Johansson, E. M. J.; Kloo, L.; Hagfeldt, A. Jen, A. K. Y.; Sun, L. *Chem*, **2017**, *2*, 676-687.
(30) Liu, J.; Wu, Y.; Qin, C.; Yang, X.; Yasuda, T.; Islam, A.; Zhang, K.; Peng, W.; Chen, W.; Han, L. *Energy. Environ. Sci.* **2014**, *7*, 2963-2967.
(31) Kazim, S.; Ramos, F. J.; Gao, P.; Nazeeruddin, M. K.; Grätzel, M.; Ahmad, S. *Energy. Environ. Sci.* **2015**, *8*, 1816-1823.
(32) Song, Y.; Lv, S.; Liu, X.; Li, X.; Wang, S.; Wei, H.; Li, D.; Xiao, Y.; Meng, Q. *Chem. Commun.* **2014**, *50*, 15239-15242.
(33) Franckevičius, M.; Mishra, A.; Kreuzer, F.; Luo, J.; Zakeeruddin, S. M.; Grätzel, M. *Mater. Horiz.* **2015**, *2*, 613-618.
(34) Zhao, X.; Zhang, F.; Yi, C.; Bi, D.; Bi, X.; Wei, P.; Luo, J.; Liu, X.; Wang, S.; Li, X. *J. Mater. Chem. A* **2016**, *4*, 16330-16334.
(35) Zhang, J.; Xu, B.; Yang, L.; Mingorance, A.; Ruan, C.; Hua, Y.; Wang, L.; Vlachopoulos, N.; Lira-Cantú, M.; Boschloo, G.; Hagfeldt, A.; Sun, L.; Johansson, E. M. J. *Adv. Energy Mater.* **2017**, *7*, 1602736
(36) Lu, H.; Ma, Y.; Gu, B.; Tian, W.; Li, L. *J. Mater. Chem. A* **2015**, *3*, 16445-16452.
(37) Jiang, X.; Yu, Z.; Zhang, Y.; Lai, J.; Li, J.; Gurzadyan, G. G.; Yang, X.; Sun, L. *Sci. Rep.* **2017**, *7*, 42564.
(38) Zhang, F.; Liu, X.; Yi, C.; Bi, D.; Luo, J.; Wang, S.; Li, X.; Xiao, Y.; Zakeeruddin, S. M.; Grätzel, M. *ChemSusChem* **2016**, *9*, 2578-2585.
(39) Liu, Y.; Hong, Z.; Chen, Q.; Chen, H.; Chang, W. H.; Yang, Y. M.; Song, T. B.; Yang, Y. *Adv. Mater.* **2016**, *28*, 440-446.
(40) Zhang, F.; Yi, C.; Wei, P.; Bi, X.; Luo, J.; Jacopin, G.; Wang, S.; Li, X.; Xiao, Y.; Zakeeruddin, S. M. *Adv. Energy Mater.* **2016**, *6*, 1600401.
(41) Li, Z. a.; Zhu, Z.; Chueh, C.-C.; Jo, S. B.; Luo, J.; Jang, S.-H.; Jen, A. K.-Y. *J. Am. Chem. Soc.* **2016**, *138*, 11833-11839.
(42) Liao, H. C.; Tam, T. L. D.; Guo, P.; Wu, Y.; Manley, E. F.; Huang, W.; Zhou, N.; Soe, C. M. M.; Wang, B.; Wasielewski, M. R.; Chen, L. X.; Kanatzidis, M. G.; Facchetti, A.; Chang, R. P. H.; Marks, T. J. *Adv. Energy Mater.* **2016**, *6*, 1600502.
(43) Huang, C.; Fu, W.; Li, C.-Z.; Zhang, Z.; Qiu, W.; Shi, M.; Heremans, P.; Jen, A. K.-Y.; Chen, H. *J. Am. Chem. Soc.* **2016**, *138*, 2528-2531.
(44) Lee, G.-Y.; Han, A.-R.; Kim, T.; Lee, H. R.; Oh, J. H.; Park, T. *ACS Appl. Mater. Interfaces* **2016**, *8*, 12307-12315.
(45) Son, S. Y.; Kim, Y.; Lee, J.; Lee, G.-Y.; Park, W.-T.; Noh, Y.-Y.; Park, C. E.; Park, T. *J. Am. Chem. Soc.* **2016**, *138*, 8096-8103.
(46) Zhang, H.; Yao, H.; Zhao, W.; Ye, L.; Hou, J. *Adv. Energy Mater.* **2016**, *6*, 1502177.
(47) Tao, C.; Neutzner, S.; Colella, L.; Marras, S.; Kandada, A. R. S.; Gandini, M.; De Bastiani, M.; Pace, G.; Manna, L.; Caironi, M. *Energy. Environ. Sci.* **2015**, *8*, 2365-2370.
(48) Abate, A.; Leijtens, T.; Pathak, S.; Teuscher, J.; Avolio, R.; Errico, M. E.; Kirkpatrik, J.; Ball, J. M.; Docampo, P.; McPherson, I.; Snaith, H. J. *Phys. Chem. Chem. Phys.* **2013**, *15*, 2572-2579.
(49) Sherwood, J.; Constantinou, A.; Moity, L.; McElroy, C. R.; Farmer, T. J.; Duncan, T.; Raverty, W.; Hunt, A. J.; Clark, J. H. *Chem. Commun.* **2014**, *50*, 9650-9652.
(50) Giovambattista, N.; Debenedetti, P. G.; Rossky, P. J. *J. Phys. Chem. B* **2007**, *111*, 9581-9587.
(51) Zhang, F.; Jespersen, K. G.; Björström, C.; Svensson, M.; Andersson, M. R.; Sundström, V.; Magnusson, K.; Moons, E.; Yartsev, A.; Inganäs, O. *Adv. Funct. Mater.* **2006**, *16*, 667-674.

For Table of Contents Only